Science of the Total Environment 954 (2024) 176286

Contents lists available at ScienceDirect

Science of the Total Environment

journal homepage: www.elsevier.com/locate/scitotenv

Mercury isotope fractionation and mercury source analysis in coal

Qingyi Cao [a,*], Guangyi Sun [a], Liyuan Liu [b], Handong Liang [c], Xuewu Fu [a], Xinbin Feng [a,*]

[a] State Key Laboratory of Environmental Geochemistry, Institute of Geochemistry, Chinese Academy of Sciences, Guiyang 550081, China
[b] College of Resources and Environment, University of Chinese Academy of Sciences, Beijing 100049, China
[c] State Key Laboratory for Fine Exploration and Intelligent Development of Coal Resources, Beijing 100083, China

HIGHLIGHTS

- Hg isotope composition indicate the sources of Hg in coal.
- The hydrothermal activity increases the Hg content and Δ^{199}Hg value in coal.
- Hg in coal mainly comes from vegetation Hg reservoir and marine Hg reservoir.

GRAPHICAL ABSTRACT

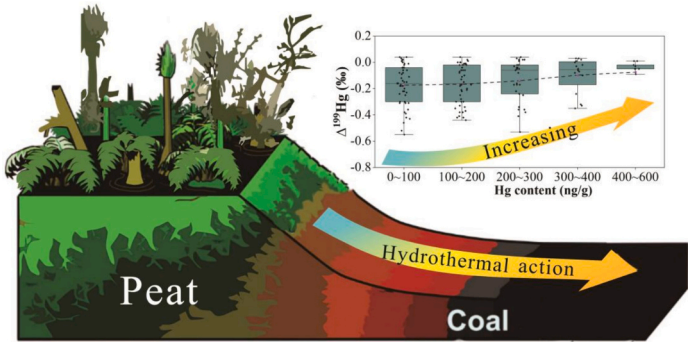

ARTICLE INFO

Editor: Sergi Diez Salvador

Keywords:
Mercury
Mercury isotope
Coal
Mass-independent fractionation

ABSTRACT

Understanding the sources of mercury (Hg) in coal is crucial for understanding the natural Hg cycle in the Earth's system, as coal is a natural Hg reservoir. We conducted analyses on the mass-dependent fractionation (MDF), reported as δ^{202}Hg, and mass-independent fractionation (MIF), reported as Δ^{199}Hg, of Hg isotopes among individual Hg species and total Hg (THg) in Chinese coal samples. This data, supplemented by a review of prior research, allowed us to discern the varying trend of THg isotope fractionation with coal THg content. The Hg isotopic composition among identified Hg species in coal manifests notable disparities, with species exhibiting higher thermal stability tending to have heavier δ^{202}Hg values, whereas HgS species typically display the most negative Δ^{199}Hg values. The sources of Hg in coal are predominantly attributed to Hg accumulation from the original plant material and subsequent input from hydrothermal activity. Hg infiltrates peat swamps *via* vegetation debris, thus acquiring a negative Δ^{199}Hg isotopic signature. Large-scale lithospheric Hg recycling *via* plate tectonics facilitates the transfer of Hg with a positive Δ^{199}Hg from marine reservoirs to the deep crust. The later-stage hydrothermal input of Hg with a positive Δ^{199}Hg enhances coal Hg content. This process has resulted in an upward trend of Δ^{199}Hg values corresponding with the increase in coal THg content, ultimately leading to near-zero Δ^{199}Hg in high-Hg coals. Coal Hg reservoirs are affected by large-scale natural Hg cycling, which involves the exchange of Hg between continents and seas.

* Corresponding authors.
E-mail addresses: qyc5411@126.com (Q. Cao), fengxinbin@vip.gyig.ac.cn (X. Feng).

https://doi.org/10.1016/j.scitotenv.2024.176286
Received 20 April 2024; Received in revised form 5 September 2024; Accepted 12 September 2024
Available online 13 September 2024

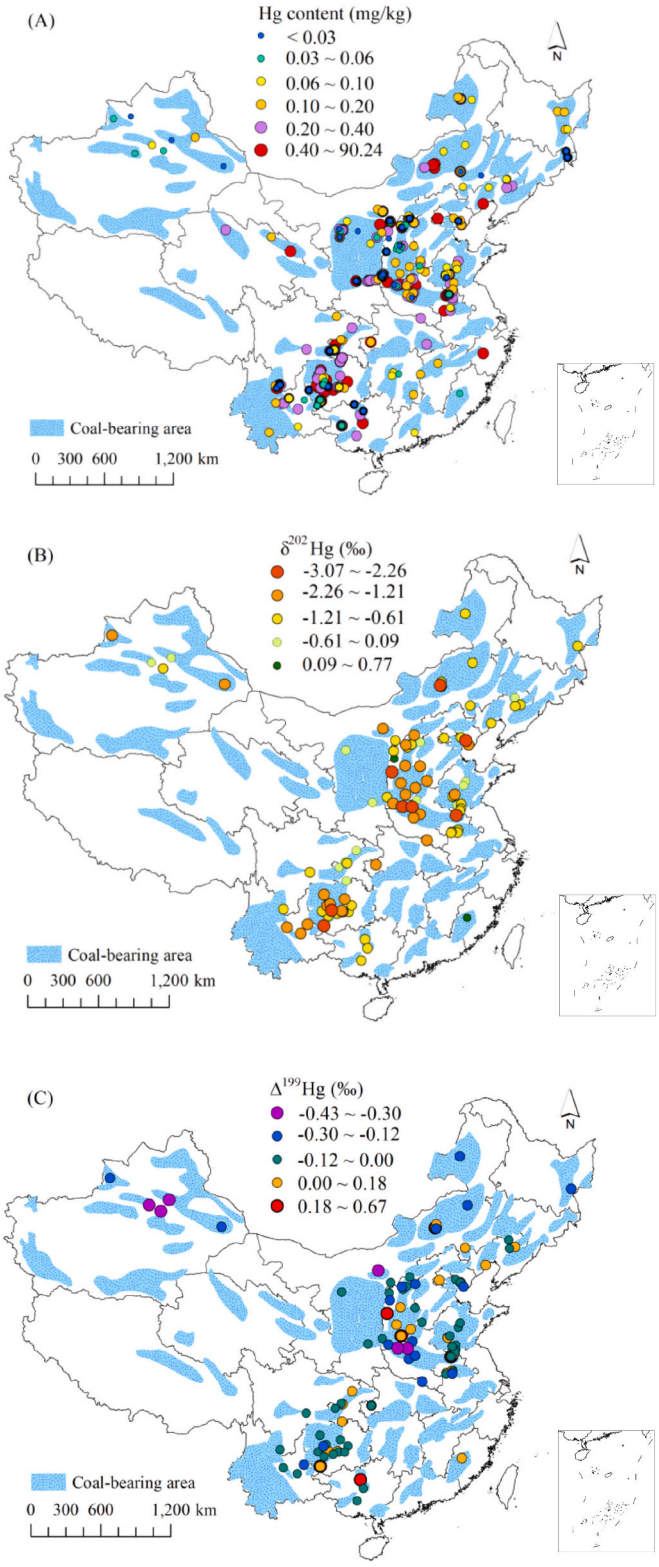

Fig. 1. Spatial distribution of Hg content, δ^{202}Hg, and Δ^{199}Hg signatures in Chinese coal. The data in the figures is from previous reports (Biswas et al., 2008; Yin et al., 2014b; Sun et al., 2014 and 2016a; Cao et al., 2021).

1. Introduction

Neurotoxic mercury (Hg) is dispersed globally *via* long-range atmospheric transport of elemental Hg (Kwon et al., 2020; Tsui et al., 2020). In addition to Hg deposits, coal deposits are the primary geological reservoirs of Hg, containing approximately 3.6 times more Hg than the average Hg concentration in the Earth's crust (Cao et al., 2021). Approximately 21 % of the estimated 2220 t global inventory of annual anthropogenic Hg emissions to the atmosphere can be attributed to coal combustion (Cao et al., 2021). A better understanding of the sources of Hg in coal, which is a significant geological reservoir for Hg, is crucial for comprehending the natural Hg cycle in the Earth system.

Stable Hg isotopes offer a perspective for studying the sources and migration processes of Hg in environmental media (Blum et al., 2014; Yin et al., 2014a; Yuan et al., 2023). Almost all physicochemical processes result in mass-dependent fractionation (MDF), whereas mass-independent fractionation (MIF) is mainly related to photo-induced reduction processes (Bergquist and Blum, 2007; Biswas et al., 2008; Buchachenko, 2018). The $\Delta^{199}Hg/\Delta^{201}Hg$ ratio is used to reflect different photodegradation and redox processes in the environment (Bergquist and Blum, 2007; Zheng et al., 2010), such as methylmercury photodegradation ($\Delta^{199}Hg/\Delta^{201}Hg \sim 1.3$) (Bergquist and Blum, 2007), gaseous Hg^0 oxidation by Br radicals ($\Delta^{199}Hg/\Delta^{201}Hg$ 1.64), gaseous Hg^0 oxidation by Cl radicals ($\Delta^{199}Hg/\Delta^{201}Hg$ 1.89) (Sun et al., 2016b), and inorganic Hg^{II} photoreduction (commonly using $\Delta^{199}Hg/\Delta^{201}Hg \sim 1.0$ as a reference (Blum and Bergquist, 2007)), with a wider range of 0.9–1.4 also being reported (Zheng and Hintelmann, 2009; Motta et al., 2020). Usually, marine Hg reservoirs (marine sediments and seawater) exhibit positive Δ^{199}Hg (Bergquist and Blum, 2007; Jackson et al., 2008), whereas terrestrial reservoirs (soil and vegetation) exhibit negative Δ^{199}Hg (Yin et al., 2010a; Demers et al., 2013; Zhang et al., 2013; Blum et al., 2014; Sun et al., 2016a; Kwon et al., 2020). Primitive earth crust and mantle have Δ^{199}Hg values close to zero (Lefticariu et al., 2011; Yin et al., 2014b; Lepak et al., 2022). These differences in Δ^{199}Hg values provides additional information for tracing the sources and fate of Hg in the environment.

The results of previous studies suggest that the Hg inventory of coal may be influenced by multiple factors, such as source areas, prevalence of coal-forming plants, paleoclimate, coalification degree, and hydrothermal action (Ren et al., 1999; Dai et al., 2012; Munir et al., 2018). However, the uncertainty associated with these factors constrain our understanding of the key sources of Hg in coal. To better understand the geochemical processes of Hg in coal deposits, we conducted analyses on the MDF (reported as δ^{202}Hg) and MIF (reported as Δ^{199}Hg) of Hg isotopes among individual Hg species and total Hg (THg) in coal samples, supplemented by a review of prior research data to discern the variation in the trend of THg isotope fractionation with coal THg content. In combination with previous research, the results of this study allow for more accurate identification of the sources of Hg in coal based on evidence from Hg isotopes.

2. Materials and methods

2.1. Analysis of Hg speciation in coal

The Hg species in coal were determined using the thermodynamic fingerprints of Hg (Biester and Nehrke, 1997; Milobowski et al., 2001; Lopez-Anton et al., 2010). This method is based on the principle that different Hg species in coal have different thermal stabilities under inert atmospheric conditions, which leads to their release and decomposition within specific temperature ranges when subjected to temperature programmed desorption (TPD) (Biester and Nehrke, 1997; Milobowski et al., 2001; Lopez-Anton et al., 2010; Rumayor et al., 2013; Rumayor et al., 2015a, 2015b, and 2015c). The stability and reproducibility of the Hg release curve for each sample were verified (Biester and Nehrke, 1997). The experimental details have been documented previously (Cao et al., 2020a and 2020b). In brief, coal samples, which were ground and sieved through a 200-mesh sieve, were subjected to analysis under an argon atmosphere, using a heating rate of 10 °C/min in the temperature range of 30–700 °C. Throughout the pyrolysis process, a Pyro-915+ pyrolyzer and a Lumex RA-915 Hg analyzer were connected in series to

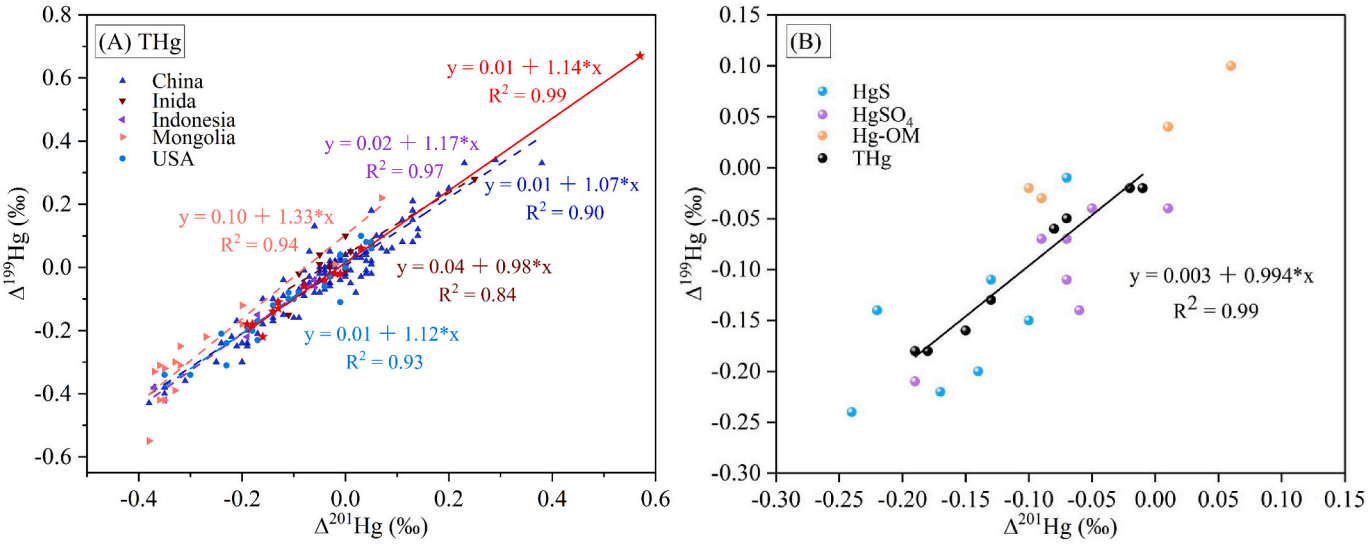

Fig. 2. Slope of Δ^{199}Hg *versus* Δ^{201}Hg in coal. The data in A is from Yin et al. (2014b), and Sun et al. (2014 and 2016a). The data in B is results of this work.

continuously monitor the atomic absorption spectroscopy (AAS) signals of Hg. The thermodynamic fingerprint properties of standard Hg compounds were used to identify Hg species in the coals, including characteristic pyrolysis intervals and Hg peaks associated with specific species. Origin software was used to deconvolve the multipeaked AAS Hg signal curve, thereby recovering the individual underlying peaks.

Eight coal samples were collected from various coal-bearing areas in China. The coal samples were numbered as follows: (1) Hami coal mine, Xinjiang Province; (2) Lvtang coal mine, Guizhou Province; (3) Chuannan coal mine, Sichuan Province; (4) Shengli coal mine, Inner Mongolia; (5) Dafang coal mine, Guizhou Province; (6) Guiding coal mine, Guizhou Province; (7) Weixin coal mine, Yunnan Province; and (8) Tangshan coal mine, Hebei Province. The coal samples were collected from underground mines and stored in sealed bags.

2.2. Hg isotope sample pre-enrichment for a single Hg species and THg

The pre-enrichment process to prepare Hg isotope samples from a single Hg species in coal was as follows. Initially, the main temperature decomposition ranges corresponding to different Hg species were determined based on the deconvolution results of the TPD-AAS Hg signal curve. To separate the thermal decomposition stages of different Hg species, the TPD heating program was modified, adding a 6-min temperature hold at the mid-temperature point where different Hg signal peaks intersected. Subsequently, TPD was performed again. A gas absorption bottle containing 5.0 mL of reverse aqua regia solution (V_{HNO_3}/V_{HCl} = 2:1) was used to capture the Hg gas released from the thermal decomposition stage of a single Hg species, completing the pre-enrichment process. The replacement of absorption bottles occurred at the end of the temperature hold stage (last 2 min) to prepare for the pre-enrichment of Hg isotope samples from the next Hg species.

Similarly, the tube furnace heating method was employed to pre-enrich Hg isotope samples of THg in coal. The coal samples were heated from 30 °C to 700 °C in an argon atmosphere at a rate of 10 °C/min, while capturing the released Hg gas with reverse aqua regia during the pyrolysis process.

2.3. Hg content and Hg isotope analysis

The THg content of the coal samples was measured using a DMA-80 Hg analyzer. Hg concentrations in the reverse aqua regia solutions were determined using a Tekran 2500 Hg analyzer, following the US-EPA method 1631 (Wang et al., 2020a, 2020b).

The Neptune Plus Multi-Collector inductively coupled plasma mass spectrometer (MC-ICP-MS) used for Hg isotopic analyses includes an online Hg^0 vapor generation system for sample introduction and a desolvating nebulizer for the Tl internal standard (NIST SRM 997) introduction (Yin et al., 2010b). The measurements were calibrated using standard-bracketing with NIST3133, following our previously published methods. The results of the MDF and MIF analyses were reported as follows (Blum and Bergquist, 2007):

$$\delta^{202}\mathrm{Hg}\ (‰) = \left[\left(^{202}\mathrm{Hg}/\,^{198}\mathrm{Hg}\right)_{\mathrm{sample}} \Big/ \left(^{202}\mathrm{Hg}/\,^{198}\mathrm{Hg}\right)_{\mathrm{NIST3133}} - 1\right] \times 1000 \quad (1)$$

$$\Delta^{xxx}\mathrm{Hg}\ (‰) = \delta^{xxx}\mathrm{Hg} - \beta_{xxx} \times \delta^{202}\mathrm{Hg} \quad (2)$$

The mass-dependent scaling factor β_{xxx} for each Hg isotope is as follows: 0.252 for ^{199}Hg, 0.502 for ^{200}Hg, and 0.752 for ^{201}Hg.

2.4. Quality assurance and quality control

The THg recovery rate in the coal samples, as determined using reverse aqua regia, was 95 ± 8 % (2σ, n = 12), thereby confirming the reliability of our Hg recovery process. The Hg isotope composition of THg derived from the Hg content and isotope data obtained during the stepwise pyrolysis process exhibited minimal deviation from the directly measured THg isotope composition (Supporting Information, Section S1). Consequently, the Hg recovery rate achieved through stepwise pyrolysis was consistent with the analytical requirements. The standard reference NIST 3177 was analyzed repeatedly to obtain the analytical uncertainty of isotopic compositions during the instrumental procedures. The isotopic compositions of NIST 3177 (δ^{202}Hg = −0.50 ± 0.08 ‰, Δ^{199}Hg = −0.01 ± 0.05 ‰, Δ^{200}Hg = 0.00 ± 0.04 ‰, and Δ^{201}Hg = −0.01 ± 0.07 ‰, 2 SD, n = 10) were in agreement with previously reported values (Fu et al., 2021; Liu et al., 2023).

3. Results

3.1. Hg isotope composition of THg in coal

The δ^{202}Hg values of THg in surveyed coal samples revealed a broad range from −1.84 to −0.62 ‰ (n = 8, Table S1). The Δ^{199}Hg values of THg ranged from −0.18 to −0.02 ‰ (n = 8). They are both distributed within the δ^{202}Hg and Δ^{199}Hg dataset range of Chinese coal (Fig. 1). The linear regression slope of Δ^{199}Hg *versus* Δ^{201}Hg for THg isotopes in the investigated coals was found to be 0.99 ± 0.07 (Fig. 2b), which is

consistent with previous observations on coal from China and other countries (Biswas et al., 2008; Yin et al., 2014b; Sun et al., 2016a). The slope of Δ^{199}Hg *versus* Δ^{201}Hg of ~1.0 is an important characteristic of THg isotopes in coal. This indicates that a portion of the Hg was subjected to photoreduction prior to being incorporated into coal.

The δ^{202}Hg and Δ^{199}Hg values of THg in Chinese coals exhibited significant variations. δ^{202}Hg values range from −3.07 to 0.92 ‰, with the average value of −1.00 ‰ (n = 122; Yin et al., 2014b; Sun et al., 2016a, 2016b). Δ^{199}Hg values range from −0.43 to 0.67 ‰, with the average value of −0.03 (n = 122). The average values are more positive than the average δ^{202}Hg (−1.16 ± 0.79 ‰) and Δ^{199}Hg (−0.11 ± 0.18 ‰) in world coal deposits (Sun et al., 2016a, 2016b). In China, Hg isotope fractionation characteristics are similar within the same coal-bearing area, whereas distinguishable differences exist between different coal-bearing areas. Outliers showing significant deviations from the typical range were observed in various regions, similar to the spatial characteristics of THg content (Fig. 1).

3.2. Hg species in coal

Distinguishable Hg compounds were observed in the studied coal samples, as evidenced by the continuous monitoring of Hg signals using TPD-AAS (Fig. 3). The Hg content of the 8 analyzed Chinese coal samples ranged from 10 to 912 ng/g, which is within the range of Hg content in most Chinese coal samples (Fig. 1A) and serves as a representative of the different levels of Hg content. Except for the No. 1 coal sample, all the samples displayed multiple peaks in the Hg signal, indicating a stepwise release Hg from individual Hg bearing species during the uniform

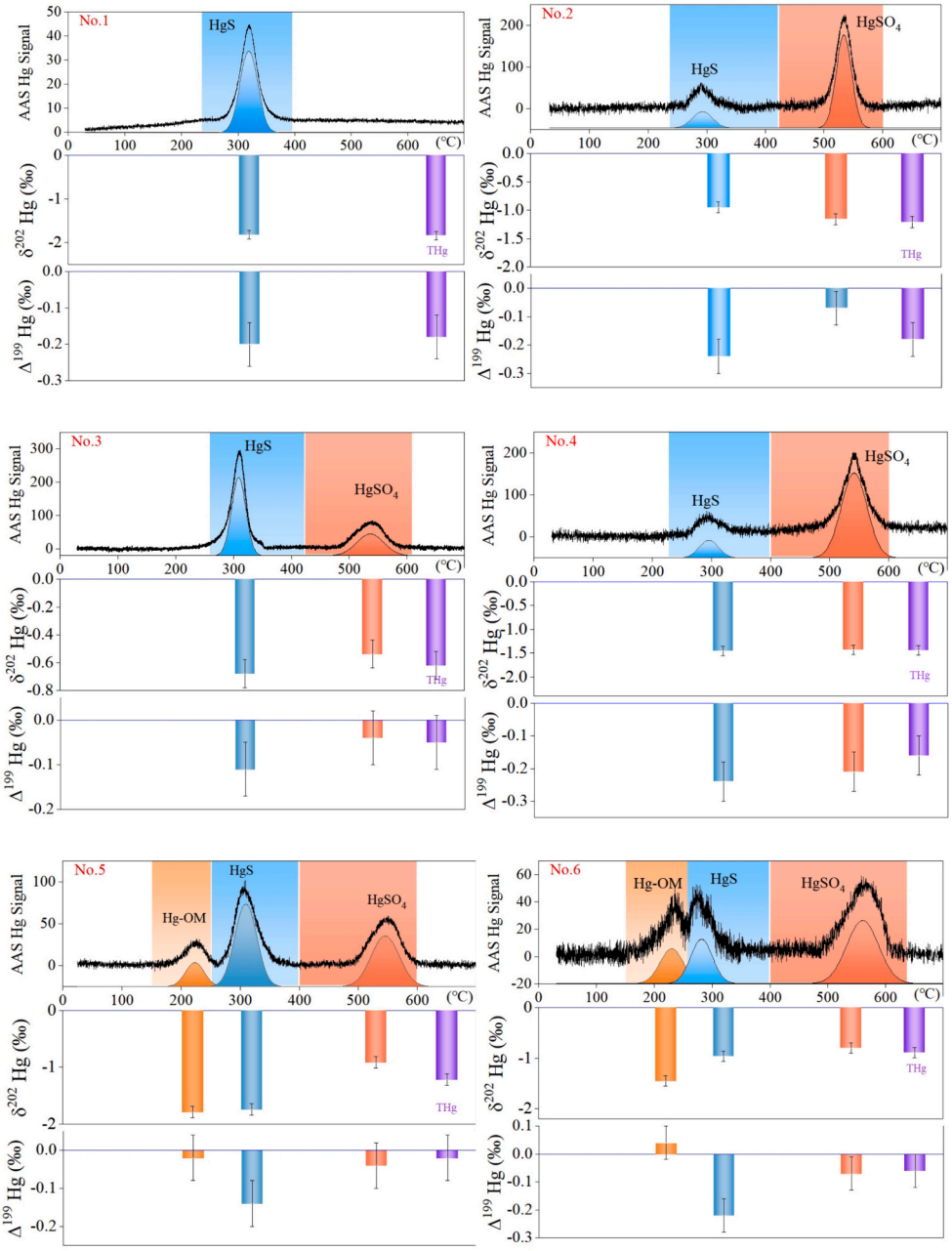

Fig. 3. The isotope composition of THg and single Hg species in coal. The top curves illustrates the continuous monitoring of AAS Hg signals (Part of the data is from Cao et al., 2020a.). The background colors correspond to the thermal decomposition ranges of different Hg species, as well as the temperature ranges used for obtaining corresponding Hg isotope samples. The color-coding of the various Hg species in the bar chart reflects their corresponding Hg isotope data. The purple bar chart represents the isotope composition of THg.

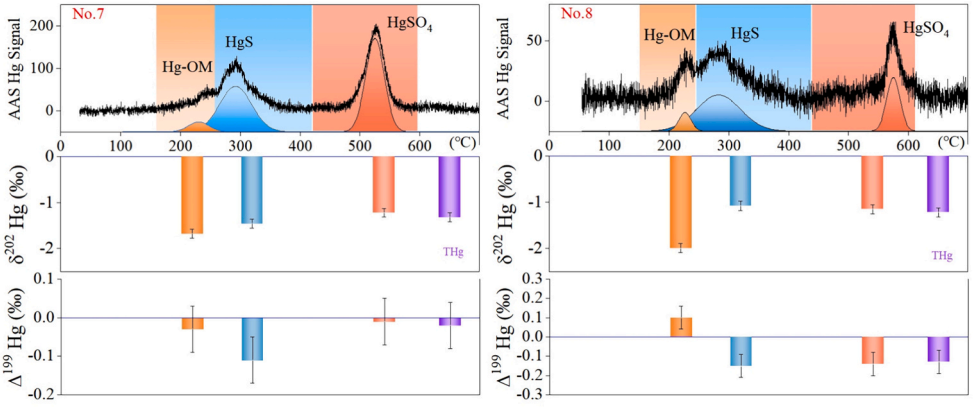

Fig. 3. (*continued*).

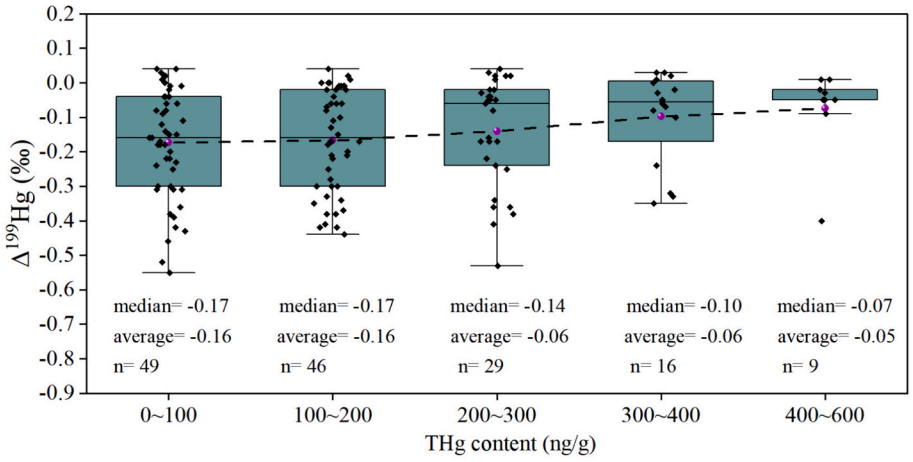

Fig. 4. Variation trends of Δ^{199}Hg in coal with THg enrichment.

temperature ramping process from 30 to 700 °C. The number and intensity of peaks in the coal samples from diverse regions exhibited variability, indicating variations in both species and Hg content. Distinct concentration peaks were observed with high frequency at central temperatures around 240, 310, and 540 °C, corresponding to temperature ranges of 200–270, 250–380, and 480–600 °C, respectively, with minor variations. Comparing the thermal fingerprint characteristics of standard Hg compounds (Milobowski et al., 2001; Lopez-Anton et al., 2010; Rumayor et al., 2013; Rumayor et al., 2015a, 2015b, and 2015c; Guo et al., 2018), the sources of Hg release within the aforementioned temperature ranges are attributed to Hg-OM (Hg bound to organic matter), HgS, and $HgSO_4$, respectively. In simpler terms, the Hg species in coal mainly include HgS, $HgSO_4$, and Hg-OM, with an average content ratio of 5 ± 7, 47 ± 27, and 47 ± 28 %, respectively.

4. Discussion

4.1. Varying trend of Δ^{199}Hg in coal with THg content

Based on previous reports on Hg isotope composition in coal (Lefticariu et al., 2011; Yin et al., 2014b; Sun et al., 2014 and 2016a), the variation patterns of Δ^{199}Hg with increasing Hg content in coal have been summarized (Fig. 4). The THg concentrations shown in Fig. 4 range from 0 to 600 ng/g, with Δ^{199}Hg values spanning from −0.55 to 0.04 ‰ and δ^{202}Hg values ranging from −3.90 to 0.70 ‰, thereby encompassing the main distribution range of Hg concentration in coal. Δ^{199}Hg exhibits an increasing trend with increasing Hg content in coal from 0 to 600 ng/g, with a rise of 0.11 ‰ (*t*-test, $p < 0.05$). This indicates that the increase in Hg content in coal is because of the replenishment of Hg inventory by the Hg source with positive Δ^{199}Hg.

Large-magnitude MIF only occurs during photochemical reactions in surface environments; thus, theoretically, the absence of light underground does not trigger MIF of Hg isotopes (Blum et al., 2014; Gao et al., 2024). Therefore, pronounced Δ^{199}Hg signals observed in various hydrothermal systems in convergent margins and intracontinental settings indicate the input of external Hg sources (Yin et al., 2023). Small and significant positive Δ^{199}Hg values have been observed in various hydrothermal systems, such as hydrothermal fluid samples (0.11–0.56 ‰; Sherman et al., 2009), Mo deposits (0.10 ± 0.07 ‰; Gao et al., 2024), and mantle (Yin et al., 2023). Recent studies have attempted to establish the geochemical cycle models to explain the deep cycling of Hg on Earth involved in large-scale translithospheric Hg exchange (Deng et al., 2021; Gao et al., 2024; Yin et al., 2023; Yin et al., 2022). In summary, marine Hg reservoirs with positive Δ^{199}Hg (such as seawater and ocean sediments) can enter continental reservoirs (*e.g.*, the crust and mantle) through subduction of the oceanic crust, and migrate upward again with magma or hydrothermal activity. Zheng et al. (2007) pointed out that the Hg content in Chinese coal increased with an increase in coal rank. The average Hg content is reflected as follows: lignite (0.09 ± 0.36 mg/kg, $n = 903$) < bituminous coal (0.3 ± 0.31 mg/kg, $n = 138$) < anthracite (0.84 ± 4.26 mg/kg, $n = 217$). A similar trend is reflected in global coal: lignite < sub-bituminous coal < bituminous coal < anthracite (Sun et al., 2016a). During the coal formation process, hydrothermal activity promotes the coal rank (Sun et al., 2016a, 2016b; Liu et al., 2020). The initial accumulation of Hg in coal is because of vegetation debris, which is characterized by negative Δ^{199}Hg

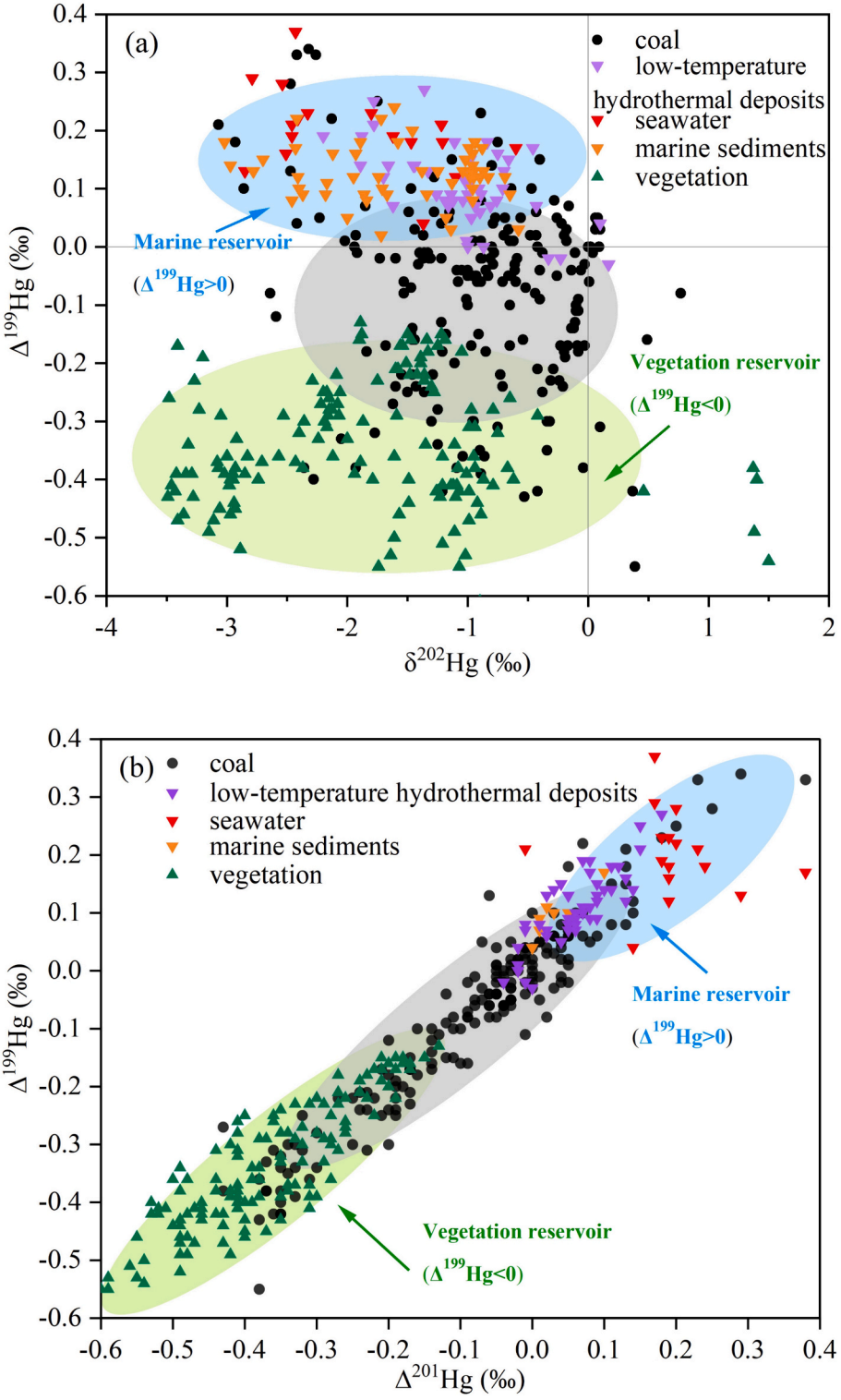

Fig. 5. Hg isotope correlation diagrams discriminate between coal, vegetation, and marine Hg reservoirs. The reference data for coal (this study and Yin et al., 2014b; Sun et al., 2016a, 2016b), vegetation (Estrade et al., 2010; Demers et al., 2013; Yu et al., 2016), seawater (Štrok et al., 2015), marine sediments (Gehrke et al., 2009; Grasby et al., 2017; Yin et al., 2017 and 2022; Yu et al., 2016), marine low-temperature hydrothermal deposits (Deng et al., 2021; Yin et al., 2022) can be found in the references.

characteristics; this original accumulation of Hg is generally low concentration. Therefore, considering the results shown in Fig. 4, we interpret the variation of Δ^{199}Hg in coal with Hg content as indicative of the Hg input caused by hydrothermal fluid with positive Δ^{199}Hg in shallow continents; the Hg in the hydrothermal systems circulates from marine reservoirs with positive Δ^{199}Hg.

The process of trace element enrichment in coal is complicated. Overall, the accumulation of elements in coal is classified into two groups: accumulation from plant material and accumulation from geological processes that occur in the peat and post-peatification stages

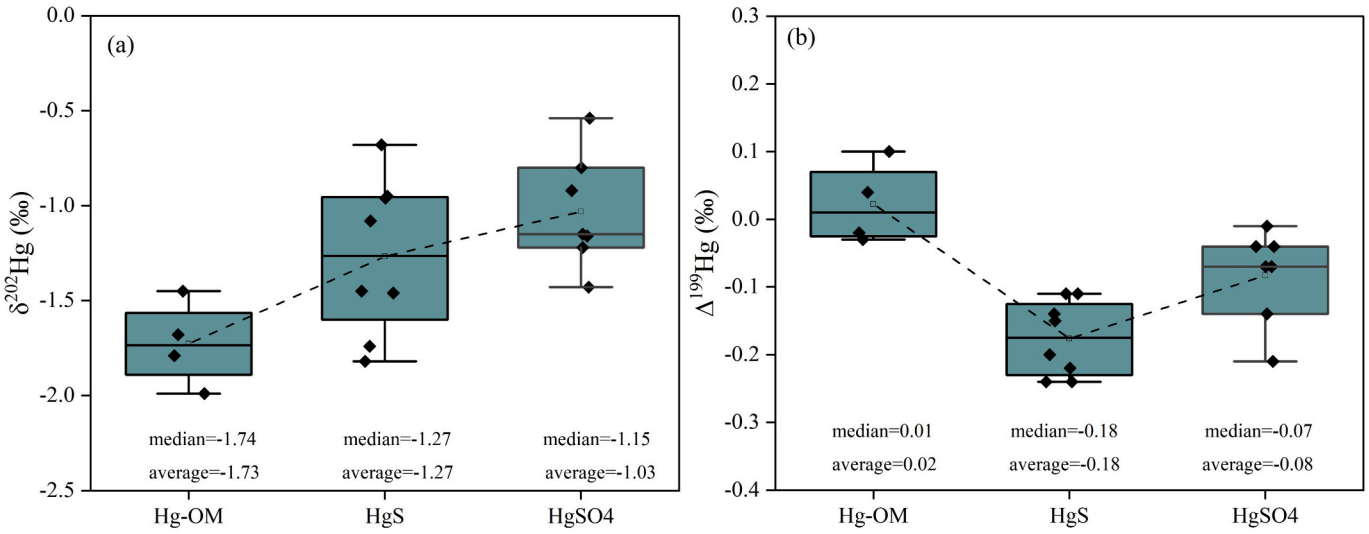

Fig. 6. Box plots showing variations of δ^{202}Hg and Δ^{199}Hg with Hg species.

(Bouška et al., 2000). The theory of coal accumulation in continental facies and transgressive processes has been utilized to elucidate coal formation patterns (Diessel, 1992). The coal reservoir showed Δ^{199}Hg/Δ^{201}Hg of ~1, indicating that it has been subjected to photoreduction process, which is consistent with the characteristics of vegetations and marine reservoirs (Fig. 5b). The photochemical reduction of Hg^{II} complexed with thiol ligands can preferentially release odd-mass-number isotopes of Hg, thereby generating negative Δ^{199}Hg in the residual fraction. This mechanism has been proposed to elucidate the development of observed negative Δ^{199}Hg signatures in Hg^{II} deposited from the atmosphere onto foliage surfaces, potentially offering a general explanation for the negative Δ^{199}Hg values observed in vegetation reservoirs (Zheng and Hintelmann, 2010; Blum et al., 2014). Conversely, the primary input of mercury into the oceans occurs *via* wet deposition of Hg^{II}, leading to positive Δ^{199}Hg values in marine reservoirs (Bergquist and Blum, 2007; Jackson et al., 2008). Typical coal deposits controlled by marine environments include the Late Permian coals from Guiding and Ziyun in Guizhou Province, Heshan in Guangxi Province, and Yanshan in Yunnan Province (Dai et al., 2012). Nevertheless, the substantial enrichment of trace elements in coal is frequently associated with the influence of epigenetic hydrothermal fluids (Dai et al., 2012). In addition, a small amount of coal samples were detected to have a significantly positive Δ^{199}Hg (Fig. 5a), which may be because of the hydrothermal fluid reaching the surface and being again affected by surface photochemical reduction (Sherman et al., 2009). Similar phenomena have been reported in the analyses of coal from China (Guizhou, Shanxi, Anhui, Inner Mongolia), India, Mongolia, Ukraine, and Romania (Transylvania) (Yudovich and Ketris, 2005a, 2005b; Biswas et al., 2008; Yan et al., 2013; Yin et al., 2014b; Sun et al., 2016a).

4.2. Hg isotope composition of the single Hg species in coal

In Fig. 3, we illustrate the δ^{202}Hg and Δ^{199}Hg of individual Hg species in the coal samples. In the case of No. 1 coal, which exhibited a single Hg component (HgS), the Hg isotope characteristics (δ^{202}Hg and Δ^{199}Hg) obtained within the temperature range of 270–380 °C (δ^{202}Hg: −1.82 ‰; Δ^{199}Hg: −0.20 ‰) highly match the isotopic characteristics of THg (obtained within 30–700 °C, δ^{202}Hg: −1.84 ‰; Δ^{199}Hg: −0.18 ‰). As for δ^{202}Hg, although significant differences were observed in THg content and its δ^{202}Hg values among all the coal samples, the trend in δ^{202}Hg signatures among different Hg species is evident. Hg species with relatively weak thermal stability tended to have lighter δ^{202}Hg values (Fig. 6a). As an example, in No. 6 coal, the first Hg species (Hg-OM), representing the least thermally stable species, exhibited the lightest δ^{202}Hg value of −1.45 ‰. The second Hg species (HgS), identified in the intermediate temperature range, showed a relatively heavier δ^{202}Hg value of −0.96 ‰. $HgSO_4$, representing the most stable species, had a heavier δ^{202}Hg value of −0.80 ‰, differing by up to 0.65 ‰. These results indicated that lighter Hg isotopes were more enriched in Hg species with weaker thermal stability in coal. Similarly, lighter Hg isotopes are preferentially released during ore roasting processes (Wiederhold et al., 2013).

For MIF, the Δ^{199}Hg value of a single Hg species might be obscured or weakened when analyzing THg isotopes. For example, in the case of No.5 coal, the Δ^{199}Hg value of THg was −0.02 ‰, without obvious MIF. However, closer examination revealed that the HgS component exhibited a clear Δ^{199}Hg value of −0.14 ‰. Similar phenomena were observed in other samples, such as samples No. 3, 6, and 7. This phenomenon is easily understood as the dilution effect of other Hg species, leading to weakening of the MIF signal intensity of individual Hg species. In most coal samples, the MIF characteristics of different Hg species within the Hg pool were not parallel. Generally, HgS exhibited significantly negative MIF characteristics, followed by $HgSO_4$, whereas the MIF of Hg-OM was not significant (Fig. 6b).

Significant correlations were observed between the Hg contents of various single Hg species and THg in coal (Table S2). The correlation coefficients between Hg-OM, HgS, $HgSO_4$, and THg are 0.99 ($p < 0.01$), 0.85 ($p < 0.01$), and 0.94 ($p < 0.01$), respectively. However, the bulk analysis results do not exhibit a clear correlation between THg content and the THg isotopic composition (δ^{202}Hg and Δ^{199}Hg). This indicates that the formation and retention mechanisms of different Hg species are inconsistent.

HgS is a Hg species present in every coal sample, displaying a more negative Δ^{199}Hg signature (Fig. 6b). A significant correlation is observed between the Δ^{199}Hg value of HgS and the Δ^{199}Hg value of THg (Table S2). This indicates that the HgS species play a key role in controlling the isotopic composition of THg in coal. Manceau et al. (2018) observed HgS nanoparticles in the intact leaves of 22 native plants in China using high-energy-resolution X-ray absorption near-edge structure spectroscopy, which accounted for 57 % of the total Hg content, while the rest were designated as dithiolate complexes ($Hg(SR)_2$). In addition, the Hg carried by hydrothermal processes into coal deposits was mainly discovered in the form of HgS, accompanied by pyrite (Yudovich and Ketris, 2005a, 2005b). Therefore, based on the previous discussion, we suggest that the HgS in low-Hg coal mainly originates from plants, whereas the addition of Hg from marine sources forms high-Hg coal, which is also added in the form of HgS. Although the addition of marine source Hg partially offsets negative Δ^{199}Hg values, the Δ^{199}Hg of

HgS remains negative, depending on the difference in Δ^{199}Hg between marine and vegetation storage and the proportion of input. For $HgSO_4$, it exhibits a slight negative Δ^{199}Hg characteristic (Fig. 6b). Cao et al. (2020b) pointed out that HgS in coal can be transformed into $HgSO_4$ during weathering. Therefore, we speculate that $HgSO_4$ was derived from partial initial HgS conversion. We cannot yet provide a clear understanding of the formation mechanism of Hg-OM because of lack of research evidence on a single Hg species in coal. This was speculated to be related to the inheritance of organically bound Hg in vegetation and the chemical fixation of weakly bound Hg by organic matter during coal formation.

5. Conclusions

Hg inventory in coal deposits is a result of the natural Hg cycle. The initial accumulation of Hg in coal originates from vegetation debris in peat swamps, with the Hg isotopic signature of negative Δ^{199}Hg. Large-scale lithospheric Hg recycling *via* plate tectonics enables the transfer of Hg with a positive Δ^{199}Hg from marine reservoirs to the deep crust. The later hydrothermal activity increased the coal rank and imported marine source Hg, resulting in the increase of Hg content and Δ^{199}Hg value in coal.

CRediT authorship contribution statement

Qingyi Cao: Writing – original draft, Methodology, Conceptualization. **Guangyi Sun:** Writing – review & editing. **Liyuan Liu:** Writing – review & editing. **Handong Liang:** Writing – review & editing. **Xuewu Fu:** Writing – review & editing. **Xinbin Feng:** Writing – review & editing.

Declaration of competing interest

The authors declare no conflicts of interest relevant to this study.

Data availability

Data will be made available on request.

Acknowledgments

This work was supported by the National Natural Science Foundation of China (No. 42407351 and 42394090) and Guizhou Provincial 2019 Science and Technology Subsidies (No. GZ2019SIG).

Appendix A. Supplementary data

Supplementary data to this article can be found online at https://doi.org/10.1016/j.scitotenv.2024.176286.

References

Bergquist, B.A., Blum, J.D., 2007. Mass-dependent and-independent fractionation of hg isotopes by photoreduction in aquatic systems. Science 318 (5849), 417–420.
Biester, H., Nehrke, G., 1997. Quantification of mercury in soils and sediments–acid digestion versus pyrolysis. Fresenius J. Anal. Chem. 358, 446–452.
Biswas, A., Blum, J.D., Bergquist, B.A., Keeler, G.J., Xie, Z., 2008. Natural mercury isotope variation in coal deposits and organic soils. Environ. Sci. Technol. 42, 8303–8309.
Blum, J.D., Bergquist, B.A., 2007. Reporting of variations in the natural isotopic composition of mercury. Anal. Bioanal. Chem. 388, 353–359.
Blum, J.D., Sherman, L.S., Johnson, M.W., 2014. Mercury isotopes in earth and environmental sciences. Annu. Rev. Earth Planet. Sci. 42, 249–269.
Bouška, V., Pesek, J., Sykorova, I., 2000. Probable modes of occurrence of chemical elements in coal. Acta Montana. Serie B, Fuel, Carbon, Mineral Processing, Praha 10, 53–90.
Buchachenko, A.L., 2018. Mercury isotopes in earth and environmental chemistry. Russian J. Phys. Chem. B 12, 635–644.
Cao, Q., Yang, L., Qian, Y., Liang, H., 2020a. Study on mercury species in coal and pyrolysis-based mercury removal before utilization. ACS Omega 5 (32), 20215–20223.
Cao, Q.Y., Qian, Y.H., Liang, H.D., Li, Z.P., Chen, S.Y., Yang, L., Zhan, Q., 2020b. Mercury forms and their transformation in pyrite under weathering. Surf. Interface Anal. 52, 283–292.
Cao, Q., Yang, L., Ren, W., Song, Y., Huang, S., Wang, Y., Wang, Z., 2021. Spatial distribution of harmful trace elements in Chinese coalfields: an application of WebGIS technology. Sci. Total Environ. 755, 142527.
Dai, S., Ren, D., Chou, C.L., Finkelman, R.B., Seredin, V.V., Zhou, Y., 2012. Geochemistry of trace elements in Chinese coals: a review of abundances, genetic types, impacts on human health, and industrial utilization. Int. J. Coal Geol. 94, 3–21.
Demers, J.D., Blum, J.D., Zak, D.R., 2013. Mercury isotopes in a forested ecosystem: implications for air-surface exchange dynamics and the global mercury cycle. Global Biogeochem. Cycles 27, 222–238.
Deng, C., Sun, G., Rong, Y., Sun, R., Sun, D., Lehmann, B., Yin, R., 2021. Recycling of mercury from the atmosphere-ocean system into volcanic-arc–associated epithermal gold systems. Geology 49 (3), 309–313.
Diessel, C.F.K., 1992. Coal-Bearing Depositional System. Springer-Verlag, Berlin.
Estrade, N., Carignan, J., Donard, O.F., 2010. Isotope tracing of atmospheric mercury sources in an urban area of northeastern France. Environ. Sci. Technol. 44 (16), 6062–6067.
Fu, X., Jiskra, M., Yang, X., Marusczak, N., Enrico, M., Chmeleff, J., Heimbürger-Boavida, L.E., Gheusi, F., Sonke, J.E., 2021. Mass-independent fractionation of even and odd mercury isotopes during atmospheric mercury redox reactions. Environ. Sci. Technol. 55, 10164–10174.
Gao, L.J., Sun, D.Y., Tian, Z.D., Luo, A.B., Lehmann, B., Yin, R.S., 2024. Positive Δ199Hg anomalies in Mesozoic porphyry Mo deposits of northeastern China and their implications to the metallogeny of arc-related hydrothermal systems at convergent margins. Chem. Geol. 645, 121880.
Gehrke, G.E., Blum, J.D., Meyers, P.A., 2009. The geochemical behavior and isotopic composition of hg in a mid-Pleistocene western Mediterranean sapropel. Geochim. Cosmochim. Acta 73 (6), 1651–1665.
Grasby, S.E., Shen, W.J., Yin, R.S., Gleason, J.D., Blum, J.D., Lepak, R.F., Hurley, J.P., Beauchamp, B., 2017. Isotopic signatures of mercury contamination in latest Permian oceans. Geology 45 (1), 55–58.
Guo, S., Zhang, L.C., Niu, X.R., Gao, L.B., Cao, Y.Z., Wei, X.X., Li, X., 2018. Mercury release characteristics during pyrolysis of eight bituminous coals. Fuel 222, 250–257.
Jackson, T.A., Whittle, D.M., Evans, M.S., Muir, D.C.G., 2008. Evidence for mass-independent and mass-dependent fractionation of the stable isotopes of mercury by natural processes in aquatic ecosystems. Appl. Geochem. 23, 547–571.
Kwon, S.Y., Blum, J.D., Yin, R., Tsui, M.T.K., Yang, Y.H., Choi, J.W., 2020. Mercury stable isotopes for monitoring the effectiveness of the Minamata convention on mercury. Earth Sci. Rev. 203, 103111.
Lefticariu, L., Blum, J.D., Gleason, J.D., 2011. Mercury isotopic evidence for multiple mercury sources in coal from the Illinois Basin. Environ. Sci. Technol. 45 (4), 1724–1729.
Lepak, R.F., Ogorek, J.M., Bartz, K.K., Janssen, S.E., Tate, M.T., Runsheng, Y., Hurley, J. P., Young, D.B., Eagles-Smith, C.A., Krabbenhoft, D.P., 2022. Using carbon, nitrogen, and mercury isotope values to distinguish mercury sources to Alaskan lake trout. Environ. Sci. Technol. Lett. 9 (4), 312–319.
Liu, X., Li, A., Ma, Z., 2020. Constraint of sedimentary processes on the sulfur isotope of authigenic pyrite. Acta Sedimentol. Sin. 38 (1), 124–137.
Liu, J., Chen, J., Poulain, A.J., Pu, Q., Hao, Z., Meng, B., Feng, X., 2023. Mercury and sulfur redox cycling affect methylmercury levels in Rice Paddy soils across a contamination gradient. Environ. Sci. Technol. 57 (21), 8149–8160.
Lopez-Anton, M.A., Yuan, Y., Perry, R., Maroto-Valer, M.M., 2010. Analysis of mercury species present during coal combustion by thermal desorption. Fuel 9, 629–634.
Manceau, A., Wang, J.X., Rovezzi, M., Glatzel, P., Feng, X.B., 2018. Biogenesis of mercury-sulfur nanoparticles in plant leaves from atmospheric gaseous mercury. Environ. Sci. Technol. 52, 3935–3948.
Milobowski, M., Amrhein, G., Kudlac, G., Yurchison, D., 2001. Wet FGD Enhanced Mercury Control for Coal−Fired Utility Boilers, Proceedings of Mega Symposium, US EPA−DOE−EPRI Combined Power Plant Air Pollutant Control Symposium: Proceedings of Mega Symposium, Chicago, IL.
Motta, L.C., Kritee, K., Blum, J.D., Tsz-Ki Tsui, M., Reinfelder, J.R., 2020. Mercury isotope fractionation during the photochemical reduction of hg (II) coordinated with organic ligands. J. Phys. Chem. A 124 (14), 2842–2853.
Munir, M.A.M., Liu, G., Yousaf, B., Ali, M.U., Abbas, Q., 2018. Enrichment and distribution of trace elements in Padhrar, Thar and Kotli coals from Pakistan: comparison to coals from China with an emphasis on the elements distribution. J. Geochem. Explor. 185, 153–169.
Ren, D., Zhao, F., Wang, Y., Yang, S., 1999. Distributions of minor and trace elements in Chinese coals. Int. J. Coal Geol. 40 (2–3), 109–118.
Rumayor, M., Diaz-Somoano, M., Lopez-Anton, M.A., Martinez-Tarazona, M.R., 2013. Mercury compounds characterization by thermal desorption. Talanta 114, 318–322.
Rumayor, M., Lopez-Anton, M.A., Diaz-Somoano, M., Rosa Martinez-Tarazona, M., 2015a. A new approach to mercury speciation in solids using a thermal desorption technique. Fuel 160, 525–530.
Rumayor, M., Diaz-Somoano, M., Lopez-Anton, M.A., Martínez-Tarazona, M.R., 2015b. Application of thermal desorption for the identification of mercury species in solids derived from coal utilization. Chemosphere 119, 459–465.
Rumayor, M., Diaz-Somoano, M., Lopez-Anton, M.A., Ochoa-González, R., Martínez-Tarazona, M.R., 2015c. Temperature programmed desorption as a tool for the identification of mercury fate in wet-desulphurization systems. Fuel 148, 98–103.

Sherman, L.S., Blum, J.D., Nordstrom, D.K., McCleskey, R.B., Barkay, T., Vetriani, C., 2009. Mercury isotopic composition of hydrothermal systems in the Yellowstone plateau volcanic field and Guaymas Basin sea-floor rift. Earth Planet. Sci. Lett. 279 (1–2), 86–96.

Štrok, M., Baya, P.A., Hintelmann, H., 2015. The mercury isotope composition of Arctic coastal seawater. Comptes. Rendus. Geosci. 347, 368–376.

Sun, R., Sonke, J.E., Heimbürger, L.-E., Belkin, H.E., Liu, G., Shome, D., Cukrowska, E., Liousse, C., Pokrovsky, O.S., Streets, D.G., 2014. Mercury stable isotope signatures of world coal deposits and historical coal combustion emissions. Environ. Sci. Technol. 48, 7660–7668.

Sun, R., Sonke, J.E., Liu, G., 2016a. Biogeochemical controls on mercury stable isotope compositions of world coal deposits: a review. Earth Sci. Rev. 152, 1–13.

Sun, G., Sommar, J., Feng, X., Lin, C.J., Ge, M., Wang, W., Yin, R.S., Fu, X.W., Shang, L.H, 2016b. Mass-dependent and-independent fractionation of mercury isotope during gas-phase oxidation of elemental mercury vapor by atomic cl and Br. Environ. Sci. Technol. 50(17), 9232–9241.

Tsui, M.T.K., Blum, J.D., Kwon, S.Y., 2020. Review of stable mercury isotopes in ecology and biogeochemistry. Sci. Total Environ. 716, 135386.

Wang, Y., Janssen, S.E., Schaefer, J.K., Yee, N., Reinfelder, J.R., 2020a. Tracing the uptake of hg (II) in an iron-reducing bacterium using mercury stable isotopes. Environ. Sci. Technol. Lett. 7 (8), 573–578.

Wang, X., Luo, J., Yuan, W., Lin, C.J., Wang, F., Liu, C., Wang, G., Feng, X., 2020b. Global warming accelerates uptake of atmospheric mercury in regions experiencing glacier retreat. Proc. Natl. Acad. Sci. U. S. A. 117, 2049–2055.

Wiederhold, J.G., Smith, R.S., Siebner, H., Jew, A.D., Brown Jr., G.E., Bourdon, B., Kretzschmar, R., 2013. Mercury isotope signatures as tracers for hg cycling at the new Idria hg mine. Environ. Sci. Technol. 47 (12), 6137–6145.

Yan, Z., Liu, G., Sun, R., Wu, D., Wu, B., Zhou, C., 2013. Mercury distribution in coals influenced by magmatic intrusions, and surface waters from the Huaibei coal Mining District, Anhui. China. Appl. Geochem. 33, 298–305.

Yin, R., Feng, X., Shi, W., 2010a. Application of the stable-isotope system to the study of sources and fate of hg in the environment: a review. Appl. Geochem. 25 (10), 1467–1477.

Yin, R.S., Feng, X.B., Foucher, D., Shi, W.F., Zhao, Z.Q., Wang, J., 2010b. High precision determination of mercury isotope ratios using online mercury vapor generation system coupled with multicollector inductively coupled plasma-mass spectrometer. Chin. J. Anal. Chem. 38 (7), 929–934.

Yin, R.S., Feng, X.B., Li, X., Yu, B., Du, B., 2014a. Trends and advances in mercury stable isotopes as a geochemical tracer. Trends Environ. Anal. Chem. 2, 1–10.

Yin, R., Feng, X., Chen, J., 2014b. Mercury stable isotopic compositions in coals from major coal producing fields in China and their geochemical and environmental implications. Environ. Sci. Technol. 48 (10), 5565–5574.

Yin, R.S., Xu, L.G., Lehmann, B., Lepak, R.F., Hurley, J.P., Mao, J.W., Feng, X.B., Hu, R. Z., 2017. Anomalous mercury enrichment in early Cambrian black shales of South China: mercury isotopes indicate a seawater source. Chem. Geol. 467, 159–167.

Yin, R., Chen, D., Pan, X., Deng, C., Chen, L., Song, X., Yu, S., Zhu, C., Wei, X., Xu, Y., Feng, X., Blum, J.D., Lehmann, B., 2022. Mantle hg isotopic heterogeneity and evidence of oceanic hg recycling into the mantle. Nat. Commun. 13 (1), 948.

Yin, X.Q., Zhao, X.F., Yin, R.S., Gao, L.J., Deng, C.Z., Tian, Z.D., Chang, S.R., Lehmann, B., 2023. Mercury isotopic compositions of iron oxide-copper-gold (IOCG) hydrothermal systems: deep hg cycling in intracontinental settings. Chem. Geol. 641, 121777.

Yu, B., Fu, X.W., Yin, R.S., Zhang, H., Wang, X., Lin, C.J., Wu, C.S., Zhang, Y.P., He, N.N., Fu, P.Q., Wang, Z.F., Shang, L.H., Sommar, J., Sonke, J.E., Maurice, L., Guinot, B., Feng, X.B., 2016. Isotopic composition of atmospheric mercury in China: new evidence for sources and transformation processes in air and in vegetation. Environ. Sci. Technol. 50, 9262–9269.

Yuan, W., Wang, X., Lin, C.J., Song, Q., Zhang, H., Wu, F., Liu, N., Lu, H., Feng, X., 2023. Deposition and re-emission of atmospheric elemental mercury over the tropical Forest floor. Environ. Sci. Technol. 57 (29), 10686–10695.

Yudovich, Y.E., Ketris, M.P., 2005a. Mercury in coal: a review: part 1. Geochemistry. Int. J. Coal Geol. 62 (3), 107–134.

Yudovich, Y.E., Ketris, M.P., 2005b. Mercury in coal: a review: part 1. Geochemistry. Int. J. Coal Geol. 62, 107–134.

Zhang, H., Yin, R., Feng, X., Sommar, J., Anderson, C.W.N., Sapkota, A., Fu, X., Larssen, T., 2013. Atmospheric mercury inputs in montane soils increase with elevation: evidence from mercury isotope signatures. Sci. Rep. 3, 1–8.

Zheng, W., Hintelmann, H., 2009. Mercury isotope fractionation during photoreduction in natural water is controlled by its hg/DOC ratio. Geochim. Cosmochim. Acta 73 (22), 6704–6715.

Zheng, W., Hintelmann, H., 2010. Isotope fractionation of mercury during its photochemical reduction by low-molecular-weight organic compounds. J. Phys. Chem. A 114, 4246–4253.

Zheng, L., Liu, G., Chou, C.L., 2007. The distribution, occurrence and environmental effect of mercury in Chinese coals. Sci. Total Environ. 384 (1–3), 374–383.

Zheng, W., Foucher, D., Hintelmann, H., 2010. Nuclear field shift effect in isotope fractionation of mercury during abiotic reduction in the absence of light. J. Phys. Chem. A 114, 4238–4245.